The background of the slide is a grayscale micrograph of a micro-robotic arm assembly. It features two vertical structures, each consisting of a rectangular top block, a thin horizontal bar, and a bundle of four thin vertical lines extending down to a rectangular base block. The structures are positioned symmetrically on either side of the central text.

**Sandia National Laboratories**  
University Alliance Design Competition

**Novel Design Category**

**Micro-robotic Arm with Thermal  
Actuator Micro-Muscle Assembly**

May 5, 2008

**University of Oklahoma**  
School of Aerospace and Mechanical Engineering

*Faculty Advisor*

Dr. Harold Stalford

*Team Members*

Kevin Bagnall  
Mangesh Edke  
Siamak Faridani  
Wade Forthman  
Joshua Homer  
Dan Garwood  
Morgan Michael

## **Abstract**

This whitepaper describes the design of a mechanical muscle powered by thermal actuators using the SUMMiT V™ fabrication process. This novel design development in MEMS technology presents a thermal actuator based micro-muscle that rotates a micro-robotic arm beyond 90 degrees. The thermal actuator muscle is comprised of two thermal actuators, a central transmission hub, rotating joint assembly, and transmission linkages. Two types of thermal actuator muscles are presented along with their design details. The thermal actuator muscle is shown to be capable of rotating a robotic arm joint beyond 90 degrees. In order to demonstrate the functionality of the micro-muscle and robotic arm, the newly designed components were placed as a tool on the operating platform designed by the University of Oklahoma 2007 MEMS team.

# Table of Contents

Abstract .....	1
Table of Contents .....	2
Objective .....	3
Introduction .....	3
Design Description .....	3
Thermal Actuators .....	3
Muscular Transmission .....	4
Thermal Actuator Linkage .....	4
Rotating Transmission Hub .....	4
Rotating Joint Linkage .....	5
Rotating Joint Assembly .....	5
Bonus Transmission Design .....	5
SUMMiT V™ Strengths .....	6
Educational Application .....	6
Principle of Operation .....	7
Operation Procedures .....	7
Measurement Procedures .....	7
Modeling .....	7
Calculations .....	7
Simulation and Animation .....	8
Thermal Actuator Simulation .....	8
Mechanism Simulation .....	8
2-D and 3-D Animation .....	8
Summary .....	9
Appendix A: References .....	10
Appendix B: Figures .....	11
Appendix C: Calculations .....	16

## Objective

The design objective is to develop a MEMS micro-muscle powered by thermal actuators that is capable of rotating a circular disk joint an angle greater than 90 degrees. The thermal actuator micro-muscle is to operate a micro-robotic arm in a stand-alone configuration or attached to an operating platform to perform tasks in and out of the plane of the chip. The design of a micro-robotic arm is to be fabricated in the SUMMiT V™ fabrication process.

## Introduction

Since the 1980s, microelectromechanical systems (MEMS) have created a new frontier for technological development. Many different disciplines of applied science and engineering are using MEMS technology, ranging from auto-manufacturing to immunology. Micro-robotics is developing as a particularly applicable area of MEMS, resulting in developments such as robotic tools to carry out micro-surgical operations and autonomous swimming robots that can administer medication to relieve obstructions in the human circulatory system. The design submitted to the University Alliance Design Competition by the University of Oklahoma team last year introduced a novel mechanism that extended operations in and out of the plane of the chip [1].

This year's design by the University of Oklahoma team install's a micro-tool on top of last year's operating plane innovation to provide a micro-robotic arm mechanism capable of performing operations above, to the side of, and in the plane of the chip. The overall chip layout is shown in Figure 1. Perhaps the potential applications of such a micro-robotic arm able to operate in three dimensions include micro-surgical operations and assembly of 3-D MEMS devices. While others have developed robotic arm devices on the centimeter scale, previous devices are significantly larger than the design developed by the University of Oklahoma team, [6], [7]. The current design has the potential of performing tasks on objects with features sizes in the nano range, considerably below the 10  $\mu\text{m}$  to 1000  $\mu\text{m}$  range. By using thermal actuators to drive the muscle mechanism, the device requires lower voltage levels than devices that use electrostatic actuation methods, [2].

## Design Description

### Thermal Actuators

The linear displacement of micro-thermal actuators is used to operate the micro-muscle design. Thermal actuators were selected over other actuation devices for their compact size, high reliability, and low voltage requirements. V-shaped thermal actuators, similar to the actuator shown in Figure 2, are placed on both sides of the arm structure to power the muscular transmission located between the actuators. Resistive heating and constrained expansion of the thermal actuator legs causes displacement of the shuttle and the linkages between the shuttle and the muscular transmission disk. The top view of the thermal actuator with 500  $\mu\text{m}$  leg lengths and offset angle of  $0.4^\circ$  developed for the micro-muscle design is shown in Figure 3.

## **Muscular Transmission**

The muscular transmission comprised of a central hub and linkages to the thermal actuators and rotating joint assembly, shown in Figures 4, 5, and 6, is the primary component of the micro-robotic arm design. The transmission converts the linear displacement of the thermal actuators into rotation of the joint assembly and its attached arm structure approximately 500  $\mu\text{m}$  from the transmission. The development of the transmission, allowing for the rotation of a small joint assembly and connected arm structure, is a novel development in MEMS technology.

## **Thermal Actuator Linkage**

The linkage between the thermal actuators and the transmission hub transfers the force output of the thermal actuators, creating a torque which causes the hub to rotate. The links (Poly 3)<sup>1</sup> have a rectangular prism shape and are attached to the thermal actuator shuttles (all Poly) and transmission hub (Poly 1+2) with pin joints. As the thermal actuator translates in one direction, the link is forced to move in the same direction and pulls on the pin joint connection to the hub. The pin joint connection on the thermal actuator shuttle prevents the link from bending and fracturing during operation. Electrical insulation between the thermal actuators and transmission hub is accomplished by separating the silicon nitride material underneath the shuttle pin joint from the substrate. The mechanical layers of the link are anchored to a Poly 0 disk that is attached to a nitride disk (separated from the substrate during the release process); the mechanical layers of the thermal actuator shuttle are anchored to Poly 0 ring around the Poly 0 disk. The separation distance of 1  $\mu\text{m}$  between the two Poly 0 structures anchored to the same nitride disk prevents electrical current from traveling from the thermal actuator to the linkage. During the release phase of the fabrication process, etching chemicals will remove the thermal oxide layer between the nitride disk and the substrate and allow the nitride disk to remain attached to the shuttle structure. Cross-sectional and 3-D views of the pin connection are shown in Figures 7 and 8.

## **Rotating Transmission Hub**

The circular transmission hub is a rotating disk with pin/rod connections to the thermal actuators and rotating joint assembly. The disk design of the transmission hub was chosen over alternate designs, such as gears, to minimize backlash and maximize the angle of rotation of the disk. Ring-shaped Poly 2 and pin joint cuts were used to separate the hub material (Poly 1+2) from the encompassing arm structure and create a bearing to hold the hub in place. Connections to the links to the thermal actuator shuttles (Poly 3) and joint assembly (Poly 4) were created with two-way bearings to allow the links to freely rotate with respect to the hub. A cross-sectional view of the transmission hub away from the pin connections to the linkages is shown in Figure 9. A detailed 3-D view of the transmission hub is shown in Figure 10.

---

<sup>1</sup> References to the polysilicon layers will be noted as “Poly” followed by the layer number.

## **Rotating Joint Linkage**

The linkage between the transmission hub and rotating joint assembly transmits rotational motion between the two parts. As the hub rotates in the counter-clockwise direction, Fig. 6, the top link is in compression and the bottom link is in tension, creating a counter-clockwise torque on the disk of the rotating joint assembly. The connections between the links and the transmission hub are constructed on the Poly 3 layer near the rotating joint assembly and Poly 4 layer near the hub, located above the thermal actuator linkage and hub itself to prevent interference between the moving parts. Interference between this linkage's pin connection (Poly 3 and 4) and the linkage between the thermal actuators and transmission hub (Poly 3) is prevented by creating a semicircular arc in the linkage between the thermal actuators and hub. To prevent against buckling of the links, the strength of the links is increased by using the other polysilicon layers (Poly 1+2 and 3) in the region between the transmission hub and the rotating joint assembly.

## **Rotating Joint Assembly**

The rotating joint assembly includes the ring-shaped bearing, its attached arm structure, and its track to hold it securely in place. Two connecting links between the transmission hub and joint bearing transmit the torque from the hub to the bearing, causing it to rotate with the hub. As the bearing rotates, its extending arm structure rotates to the same angle. The bearing is constructed using a ring-shaped pin joint cut that separates the Poly 1+2 layer material, forming the bearing structure from the Poly 1 bearing track. The bearing track is formed by two ring-shaped cuts in the sacrificial oxide material between the Poly 0 and Poly 1 layers on the inside and outside of the pin joint cut. Separation of the silicon nitride material underneath the rotating joint assembly from the substrate provides the additional layer needed to connect the bearing track to the arm structure containing the transmission and thermal actuators. A cross-sectional view of the joint assembly is shown in Figure 11. A 3-D view of the joint assembly is shown in Figure 12.

## **Bonus Transmission Design**

In the bonus design transmission design, the thermal actuators were modified to incorporate a different linkage system to the transmission hub. The advantage of this design over the original design is that the linkages between the thermal actuators and transmission hub are in tension and compression for both rotation directions of the hub. In the original design, these linkages are in tension during counter-clockwise rotation of the hub and in compression in the clockwise rotation direction. Though the linkages are designed to withstand the compressive stresses associated with this clockwise rotation, the bonus design strengthens the linkages during both clockwise and counter-clockwise rotations. Top and 3-D views of the bonus transmission design are shown in Figures 13 and 14.

Modification of the thermal actuators as a part of the bonus design includes a redesign of the pin joint connection between the thermal actuator shuttles and the linkages to the transmission hub. The linkages between corresponding thermal actuator legs on opposite sides of the arm structure function as the shuttle connecting these legs. Therefore, the connections between pairs of legs on each side of the arm structure and their linkages are independent and prevented from

interfering with one another by an offset distance between the shuttles. A top view of the pin connections used in the bonus design is shown in Figure 15.

The connection to the transmission hub in the bonus design is different than the original design due to the presence of a total of four links to the thermal actuators. A yoke shaped linkage provides the connection to the pin on the transmission hub, as shown in Figure 16. The removal of sacrificial oxide anchors the Poly 3 arm to the hub (Poly 2). A cross-sectional view of the yoke shaped linkage and pin connection to the transmission hub is shown in Figure 17.

## **SUMMiT V™ Strengths**

Unlike other MEMS fabrication processes, SUMMiT V™ provides the multiple, independent layers needed for the thermal actuator micro-muscle design along with small structural feature sizes. Because the thermal actuator micro-muscle design includes several connected translating and rotating parts, different independent layers are required for each part to prevent binding. The silicon nitride layer on the substrate of SUMMiT V™ is specifically used in the thermal actuator micro-muscle design to insulate the thermal actuator shuttle from the muscular transmission. Geometries in the silicon nitride removal layer are used in coordination with Poly 0 to create areas in which the substrate is exposed to wet etching chemicals in the release process. These etching chemicals will remove the thermal oxide layer between the substrate and silicon nitride layer, allowing the silicon nitride layer to remain attached to the polysilicon structural layers after release.

The small feature size and high precision of the SUMMiT V™ process minimizes the backlash between the transmission hub and its linkages and maximizes the range of motion of the transmission. The backlash in the thermal actuator micro-muscle depends upon the 0.3  $\mu\text{m}$  thickness of the SacOx2 layer that results in 0.3  $\mu\text{m}$  spacing in each of the pin joints. The maximum shuttle displacement of 20  $\mu\text{m}$ , which is restricted by the length of the thermal actuator legs and temperature at which the material deforms plastically, requires that the connections between the hub and links are located as close to the center of the hub as possible. The small feature size allows these pin joint connections to be close to the center and results in a large rotation angle for the relatively small thermal actuator displacements. Similarly, the feature size defines the minimum spacing between the inner and outer diameter of pin joints used to connect the links and the hub in the muscular transmission. With the small feature size provided by the SUMMiT V™ process, the muscular transmission responds quickly to thermal actuation and gives the operator more accurate control of its motion.

## **Educational Application**

The micro-robotic arm will be effective in MEMS education at the K-12 level primarily because of its relative simplicity. Children of any age will be able to understand the basic concept of an arm, especially with the similarity in the actions between the MEMS micro-muscle and a human muscle. Both utilize expansion and contraction when changing the angle of the arm. Older students will be able to understand how the micro-robotic arm functions from their prior experience with similar non-MEMS machinery, such as those used in automobile assembly lines.

The possible applications of the device would also be an effective teaching tool, by showing students the value of MEMS technology.

## **Principle of Operation**

### **Operation Procedures**

The thermal actuators used in the design require direct current electrical power to displace links connected to the transmission hub. As the thermal actuator legs heat up and expand as the current flows through them, the transmission hub rotates and causes the extending arm structure to rotate. The desired angle of rotation of the extending structure is expressed in terms of the current supplied to the thermal actuators in Appendix C. To rotate the extending arm structure to a specific angle, the operator needs to steadily apply the appropriate amount of current using a DC power supply with a current limiter. To move the forearm structure to a new angular position, the current needs to be adjusted to the corresponding value described by the plot of angle of rotation versus applied current in Appendix C. The thermal actuator simulation data given in Appendix C was provided to the design team by Michael Baker of Sandia National Laboratories.

### **Measurement Procedures**

The operation of the device will be performed using a standard probe station equipped with an optical microscope. The angle of rotation of the extending arm structure is the primary variable measured. The operator of the micro-robotic arm and independent thermal actuator micro-muscles will be able to determine the angle of rotation of the micro-robotic arm visually using the angle scale (Poly 0) constructed on the chip.

In addition several additional objects were designed and placed on the chip for interaction with the micro-robotic arm configured with the operating platform designed by the 2007 University of Oklahoma team. The ability of the operator to precisely manipulate the objects demonstrates the angle of rotation of the extending arm structure and the types of tasks that the micro-robotic arm can perform.

## **Modeling**

### **Calculations**

Based upon simulations of the thermal actuator design provided by Michael Baker, a relationship was developed between the shuttle displacement of the thermal actuators and the rotation angle of the joint assembly. Because the shuttle displacement is controlled by the current supplied to the thermal actuators, this relationship was extended to express the rotation angle of the joint assembly in terms of the electrical current. The plots of rotation angle versus shuttle displacement and rotation angle versus applied current and voltage are shown in the appendices along with the thermal actuator simulation data in Appendix C. The temperature at which plastic deformation begins limits the amount of current that can be safely applied and the resultant

displacement of the thermal actuator shuttle. The maximum displacement of the thermal actuators used in this design was determined to be approximately 20  $\mu\text{m}$ . The muscular transmission was shown to be able to rotate beyond an angle of 90 degrees as desired. The required values of thermal actuator displacement, applied current, and applied voltage required to achieve 90 degrees of rotation were calculated to be 17  $\mu\text{m}$ , 31 mA, and 10.3 V. To determine the positioning accuracy of the micro-robotic arm, the backlash in the muscular transmission was calculated to be approximately 5.8 degrees, as shown in Appendix C. The positioning error of the micro-robotic arm could be reduced by reducing the thickness of the SacOx 2 layer. The plot of the positioning error versus the thickness of the SacOx 2 layer is shown in Appendix C in order to illustrate the possible reduction in position error.

## **Simulation and Animation**

One of the key tasks in this project was to verify the mechanism design through simulation. Depending upon the problem type, structural, multi-physics, or motion simulations are performed. The main objective for performing simulations was to verify operation of mechanisms and structural integrity of critical components. Simulations also help present the design ideas unambiguously. In this project, AutoCAD along with SANDIA MEMS Design and Visualization tools is used for design, Pro/ENGINEER is used for 3-D modeling, Pro/Mechanism is used for motion simulation, and ANSYS is used for structural and multi-physics simulation. To better communicate the designs a number of 3-D animations are made using CARRARA package.

### **Thermal Actuator Simulation**

Pro/Mechanism only allows motion of rigid bodies. Hence motion induced by thermal actuators cannot be modeled in Pro/Mechanism as that motion will require modeling of the expansion of thermal actuators due to applied electric current. To overcome this problem, a separate multi-physics analysis of the thermal actuators is performed in ANSYS. The response (expansion) of thermal-actuators to applied electricity is measured and that data is exported in a table format. This data can then be used to determine motion of the tip of the thermal actuators.

### **Mechanism Simulation**

The robotic arm, mounted on the operating platform in two different configurations, is similar to the human arm. The thermal actuator muscle rotates a shoulder-like joint in both configurations with the operating platform. A sample model of the rotating shoulder joint configuration is shown in Figure 18.

### **2-D and 3-D Animation**

In order to communicate different mechanisms, one of the important tasks in this project was preparing explanatory animations. Because of ease of use and portability, Adobe Flash can be used for developing 2-D animation. Additionally, SUMMiT V™ models can be imported directly into Flash to animate.

CARRARA is used for 3-D animations, it has superior VET rendering abilities and SUMMiT V™ SAT files can be imported directly to this software without using a third party converter. 3-D animations and renderings explain the arm mechanism and help the team members communicate the designs better. 3-D animations also provide a better visualization than SUMMiT V™ layer view and help the designers visualize MEMS mechanisms. An animation of the contact springs used in the design created by the University of Oklahoma team last year is shown in Figure 19 to illustrate 2-D animations of the design.

## **Summary**

The design presented in this whitepaper for a thermal actuator micro-muscle to operate a micro-robotic arm is innovative and widely applicable to micro-robotics technology. The design is especially well-suited to the SUMMiT V™ fabrication process due to the need for multiple mechanical layers and electrical insulation in the device. Unlike more abstract MEMS devices, the thermal actuator micro-muscle and robotic arm is an ideal educational tool because its usefulness is easily seen by elementary school and postsecondary students alike.

## Appendix A: References

- [1] Z. Butler, S. Camp, J. Dingeldein, A. Mann, S. Thompson, and A. Watt, “Parvissimus Bracchius,” Sandia National Laboratories University Alliance Novel Design Competition, Apr. 2007.
- [2] M. S. Baker, R. A. Plass, T. J. Headley, and J. A. Walraven, , “Compliant Thermo-mechanical MEMS Actuators,” Sandia National Laboratories, Albuquerque, New Mexico, Tech. Rep. LDRD #52553, SAND2004-6635, Dec. 2004.
- [3] “SUMMiT V™ Five Level Surface Micromachining Technology Design Manual,” Version 1.3, MEMS Devices and Reliability Physics Department, Microelectronics Development Laboratory, Sandia National Laboratories, Albuquerque, New Mexico, Sept. 22, 2005.
- [4] B. J. Hamrock, S. R. Schmid, and B. Jacobson, “Fundamentals of Machine Elements,” 2<sup>nd</sup> ed., New York: McGraw-Hill, 2005.
- [5] J. M. Gere, “Mechanics of Materials,” 6<sup>th</sup> ed., Belmont, CA: Brooks/Cole-Thomson Learning, 2004.
- [6] J. Peirs, D. Reynaerts, and H. Van Brussel, “A Micro Robotic Arm for a Self Propelling Colonoscope,” in *Proc. Acuator 98, 6<sup>th</sup> International Conference on New Actuators*, 1998, pp. 576-579.
- [7] J.P. Merlet, ERCIM News No. 42, “The Design of the MIPS Micro-Robot for Endoscopy Applications,” Jul. 2000,  
[http://www.ercim.org/publication/Ercim\\_News/enw42/merlet.html](http://www.ercim.org/publication/Ercim_News/enw42/merlet.html).

## Appendix B: Figures

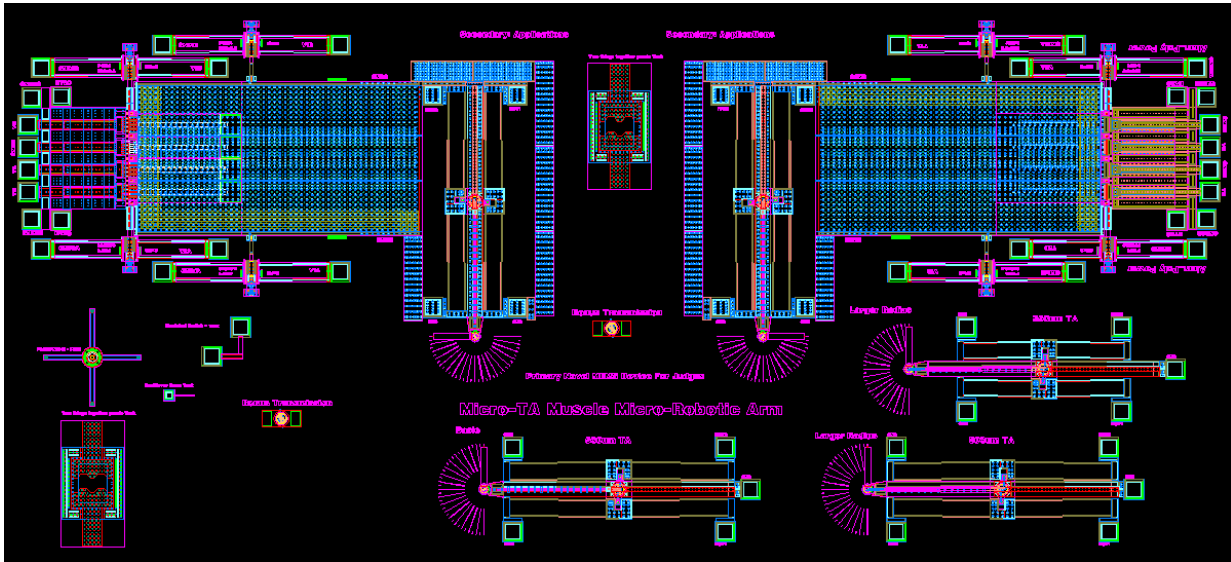


Figure 1: Overall Chip Layout

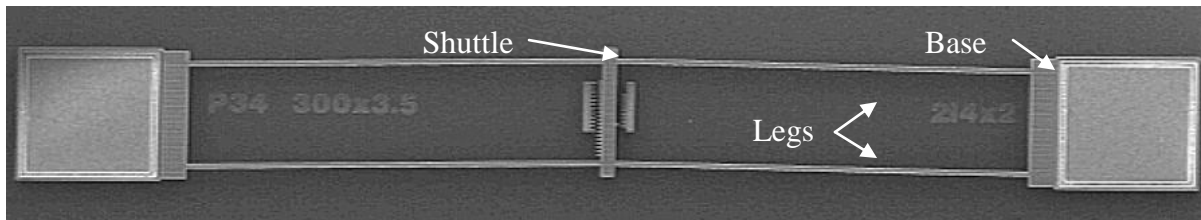


Figure 2: SEM Image of V-shaped Thermal Actuator [2]

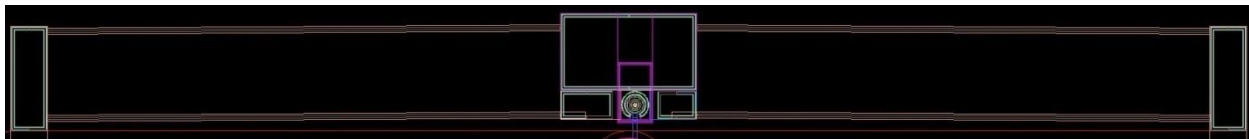


Figure 3: Top View of Thermal Actuator Design

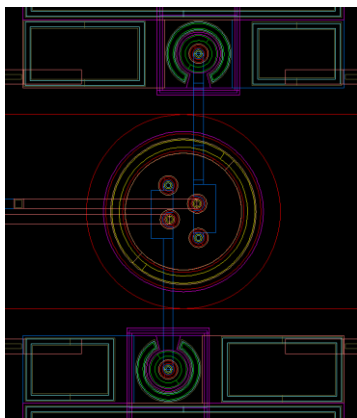


Figure 4: Top View of Muscular Transmission Design

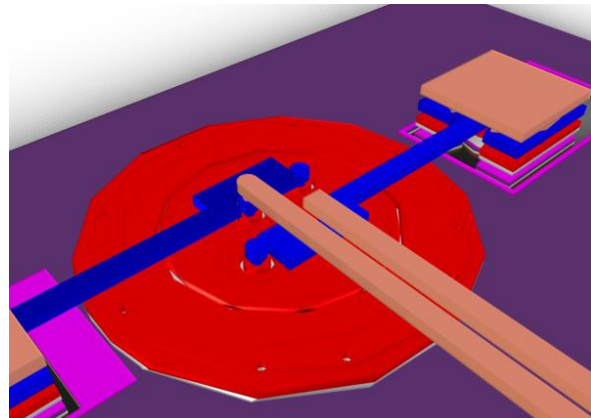


Figure 5: 3-D View of Muscular Transmission Design

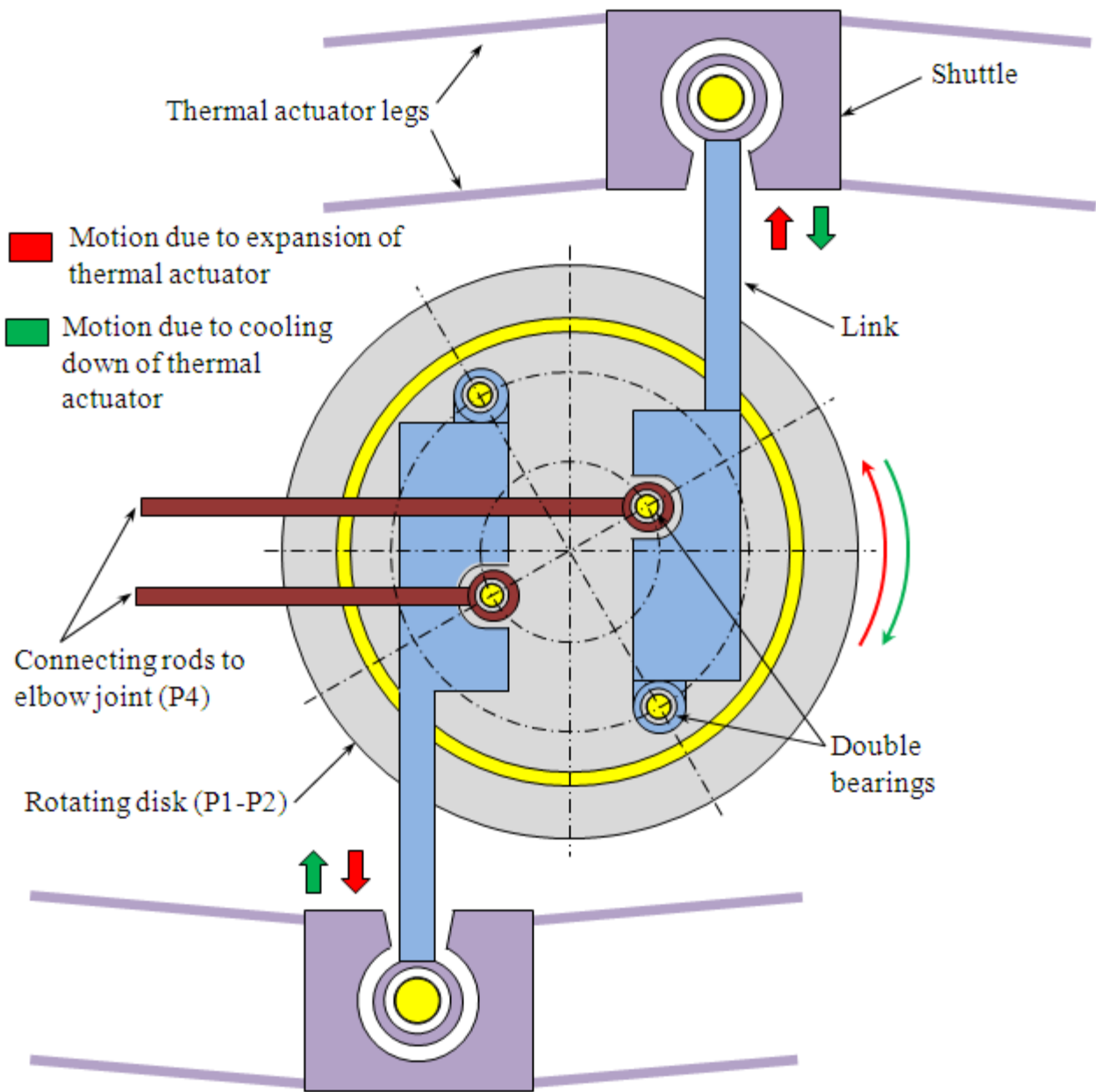


Figure 6: Schematic Diagram of the Muscular Transmission

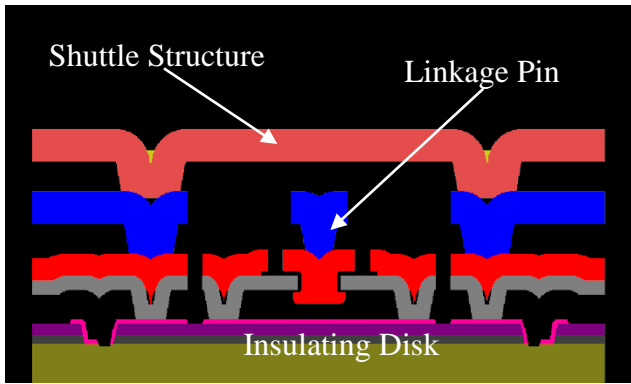


Figure 7: Cross-sectional View of Thermal Actuator Linkage Pin

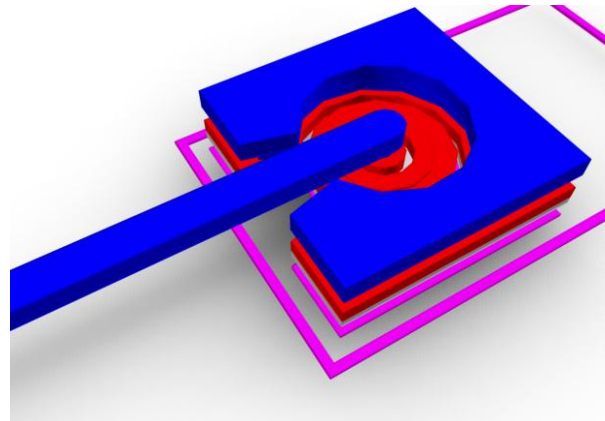


Figure 8: 3-D View of Thermal Actuator Linkage Pin

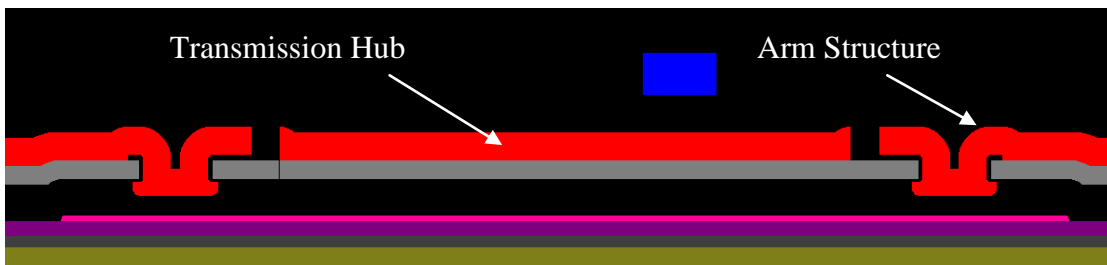


Figure 9: Cross-sectional View of Transmission Hub

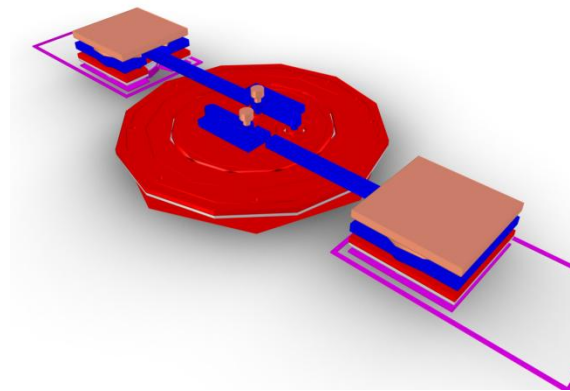


Figure 10: 3-D View of Transmission Hub

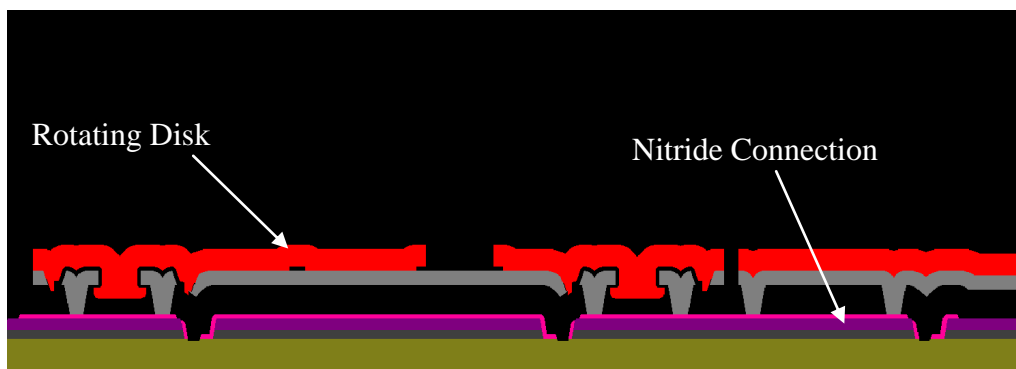


Figure 11: Cross-sectional View of Rotating Joint Assembly

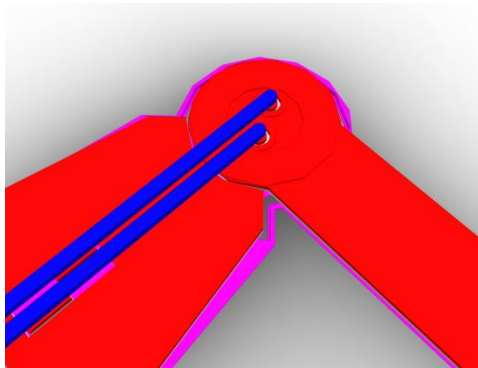


Figure 12: 3-D View of Rotating Joint Assembly

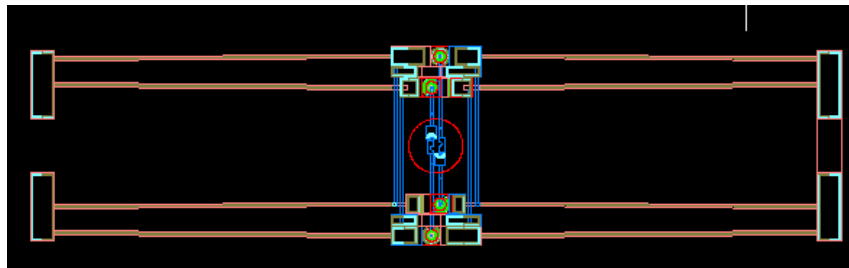


Figure 13: Top View of Bonus Transmission Design

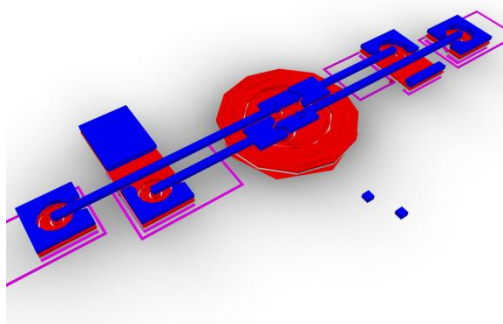


Figure 14: 3-D View of Bonus Transmission Design

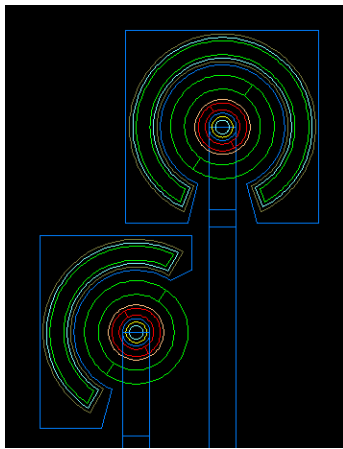


Figure 15: Top View of Thermal Actuator Linkage Pins for Bonus Design

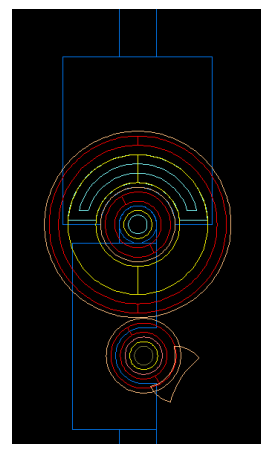


Figure 16: Top View of Three-way Bearing for Transmission Linkage for Bonus Design

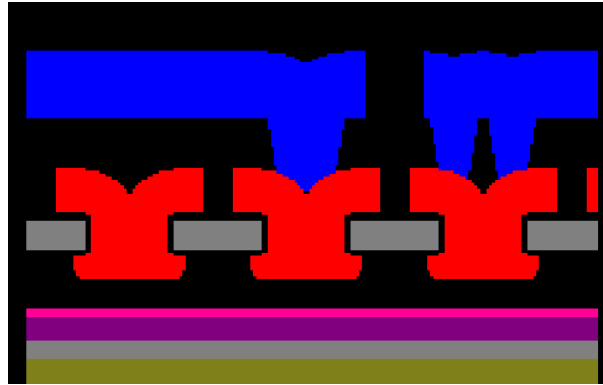


Figure 17: Cross-sectional View of Three-way Bearing for Transmission Linkage for Bonus Design

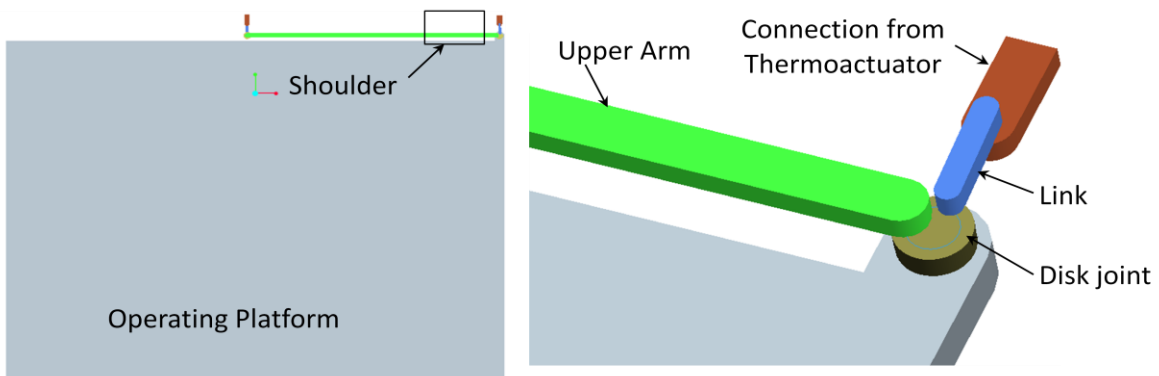


Figure 18: Pro/Engineer Model of Robotic Arm

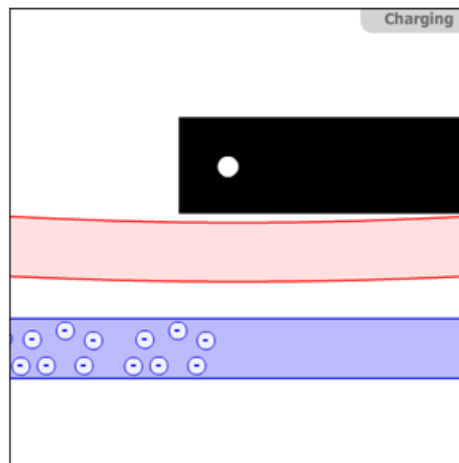
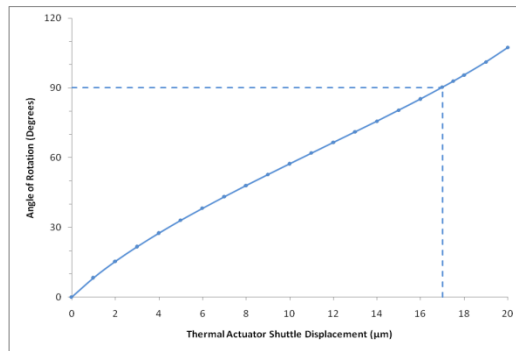


Figure 19: Sample Flash Animation of the Contact Springs for 2007 OU Design

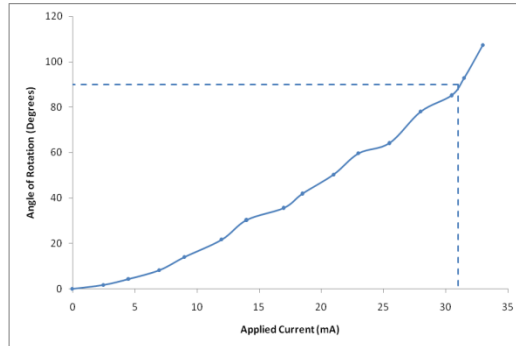
# Appendix C: Calculations

## Relationship between Angle of Rotation and Thermal Actuator Displacement and Current

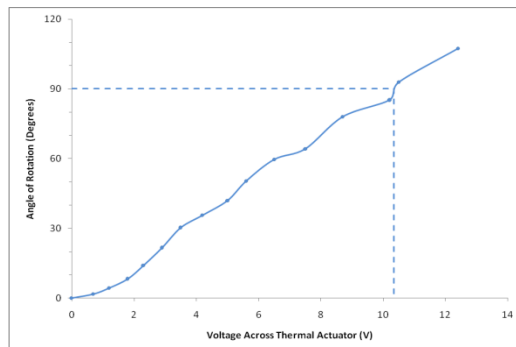
The plots of angle of rotation versus the displacement of the thermal actuator shuttle, applied current and applied voltage are shown in the figures below. The relationship between the thermal actuator displacement, applied current, and voltage was determined from simulation data provided by Michael Baker of Sandia National Laboratories. The dotted lines in the figures below represent the displacement, current, and voltage of 17  $\mu\text{m}$ , 31 mA, and 10.3 V required to achieve a rotation of 90 degrees. The calculations reflected by the figures below do not take backlash due to the 0.3  $\mu\text{m}$  pin joint spacing into consideration.



**Plot of Angle of Rotation versus Thermal Actuator Shuttle Displacement**



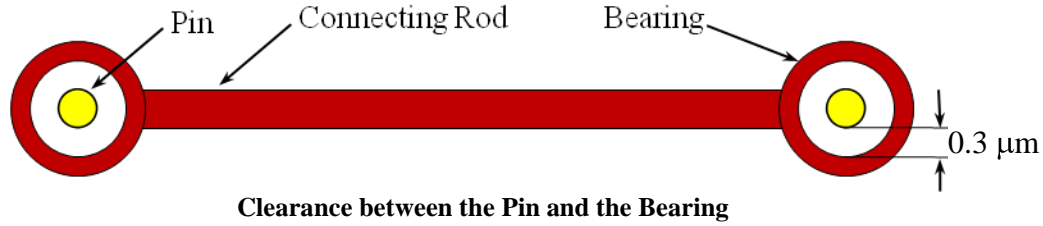
**Plot of Angle of Rotation versus Applied Current**



**Plot of Angle of Rotation versus Applied Voltage**

## Calculation of Positioning Accuracy

There are several pin joints in the robotic arm mechanism. There is a clearance of  $0.3 \mu\text{m}$  between a pin and an inner race of a bearing. As seen in the following figure, this results in some play, which affects positioning accuracy of the robotic arm. The calculations made here take maximum possible play into account for each individual joint. In actual case, the error will be less than this result.



### Step 1:

The link engages with the disk only after the thermal actuator shuttle moves by  $0.3 \mu\text{m}$ . This changes the initial angle of  $\theta_1$  (which is  $60^\circ$ ) to  $\theta'_1$  and introduces an error of  $\Delta\theta_1$ .

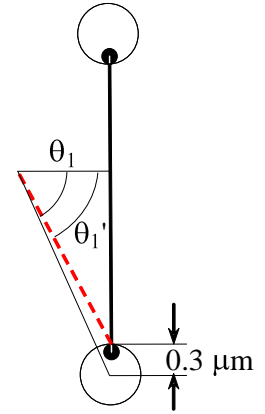
$$\Delta\theta_1 = \theta_1 - \theta'_1$$

$$\theta'_1 = \tan^{-1}\left(\frac{12.5 \sin 60^\circ - 0.3}{6.25}\right) = 59.30^\circ$$

$$\therefore \Delta\theta_1 = 0.70^\circ$$

Due to this angle, the effective distance of the pin from the disk center changes to

$$R = 6.25 / \cos \theta'_1 = 12.24 \mu\text{m}$$



**Step 1 of Accuracy**

### Step 2:

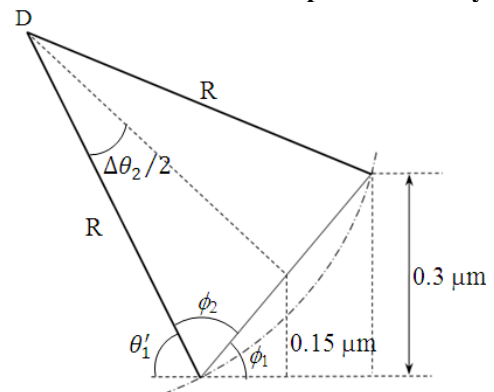
When the thermal actuator shuttle further pulls the link, the disk starts rotating. When it rotates through a certain angle and the end of the link moves vertically through  $0.3 \mu\text{m}$ , the disk engages with connecting rods. The angle through which the disk has to rotate to gain this vertical displacement of  $0.3 \mu\text{m}$  is another error,  $\Delta\theta_2$ .

$$\sin\left(\frac{\Delta\theta_2}{2}\right) = \frac{c}{R} \quad \therefore c = R \sin\left(\frac{\Delta\theta_2}{2}\right)$$

$$\sin(\phi_1) = \frac{0.15}{c} \quad \therefore \sin(\phi_1) = \frac{0.15}{R(\Delta\theta_2/2)}$$

Also, from the adjoining figure,

$$\theta'_1 + \left(90^\circ - \frac{\Delta\theta_2}{2}\right) + \phi_1 = 180^\circ$$



**Step 2 of Accuracy Calculations**

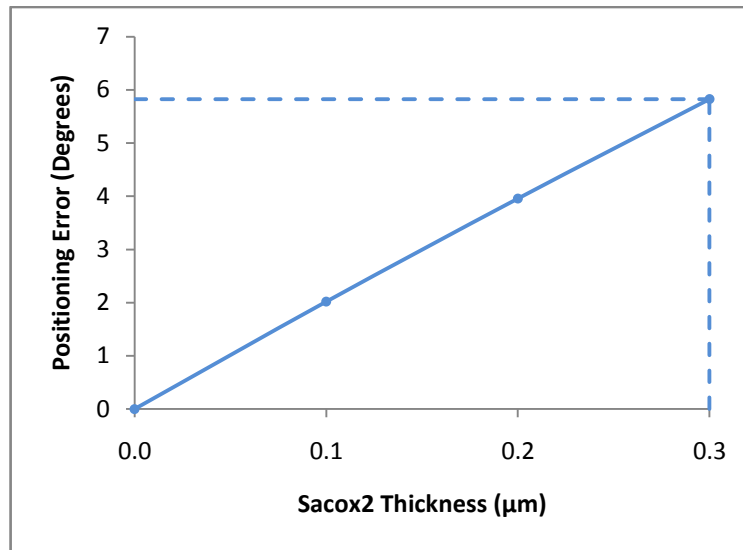
Solving the last two equations simultaneously,

$$\Delta\theta_2 = 5.11^\circ$$

Total positioning error is given by

$$\Delta\theta = \Delta\theta_1 + \Delta\theta_2 \approx 5.81^\circ$$

In order to reduce the positioning error associated with the operation of the micro-robotic arm, the thickness of the SacOx 2 layer present in all two-way bearings could theoretically be reduced. The figure below shows a plot of the positioning error in degrees versus the thickness of the SacOx 2 layer. The dotted lines shown in the figure below indicate the positioning error of  $5.8^\circ$  at a standard SacOx 2 thickness of  $0.3 \mu\text{m}$ .

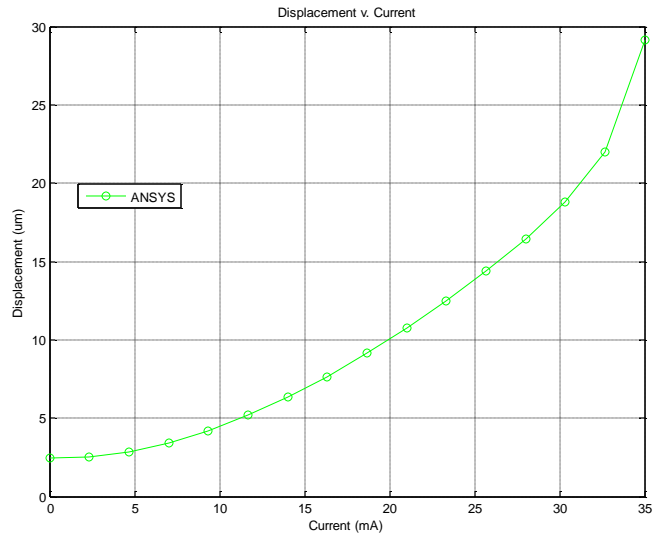


Plot of Positioning Error versus SacOx 2 Thickness

### Thermal Actuator Data

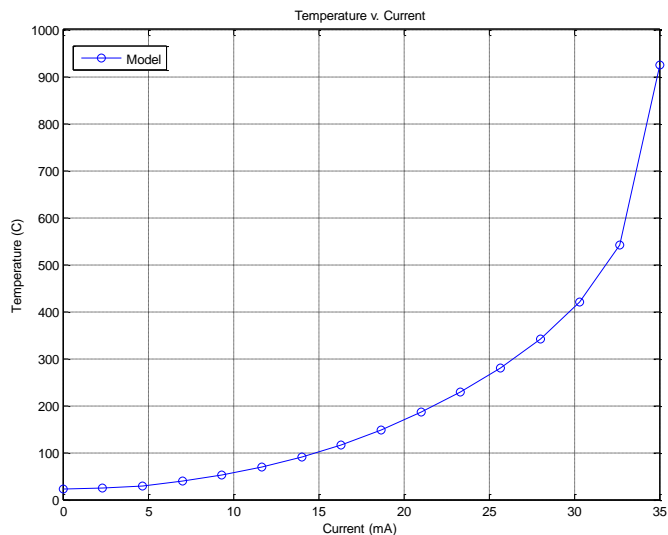
The following figures were created and provided by Michael Baker of Sandia National Laboratories for the thermal actuator geometry used in the muscle design.

The displacement shown on the vertical axis in the figure below represents the displacement of the shuttle of the thermal actuator from its initial position due to the application of the specified current. The displacement-axis intercept of  $2.5 \mu\text{m}$  illustrates that the shuttle of the thermal actuator was displaced that distance during the fabrication process. The displacement values used to generate the plot of angle of rotation of the muscular transmission versus applied current takes this offset displacement into account.



**Plot of Thermal Actuator Shuttle Displacement versus Applied Current**

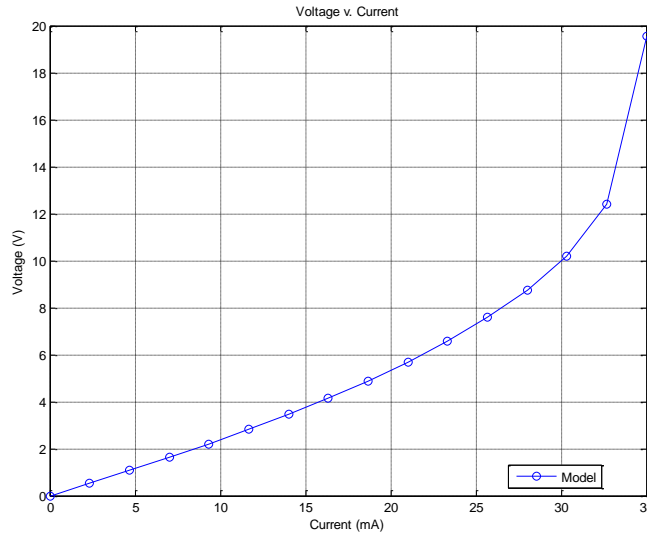
The plot of thermal actuator temperature versus applied current shown in the figure below establishes a critical parameter for the operation of the thermal actuator muscle. Polysilicon begins to deform plastically at a temperature of about 600°C; this temperature value represents the maximum temperature and maximum corresponding current that may be applied to ensure long-term reliability of the device. It is recommended that no greater than 33 mA of current be applied to the device during operation.



**Plot of Thermal Actuator Temperature versus Applied Current**

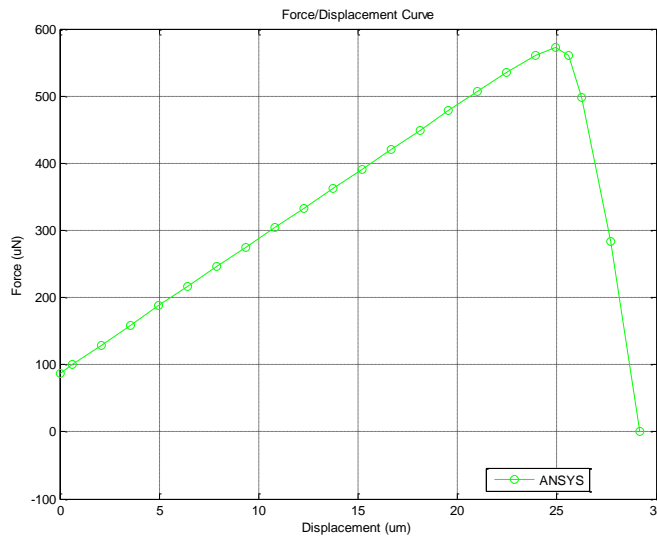
The plot of the applied voltage across the thermal actuator versus current is shown in the figure below to aid with the operation of the thermal actuator muscle. The DC power supply used to operate the device requires voltage input and current limit values. The voltage values indicated by the vertical axis in the figure below result in the applied current values indicated on the

horizontal axis of the same figure for the thermal actuator geometry used in the design. Therefore, to rotate the extending arm structure to a desired angle described by the plot of the angle of rotation versus applied current, the operator would input the appropriate voltage value given in the figure below.



**Plot of Voltage Across Thermal Actuator versus Applied Current**

The plot of the force output of the thermal actuator versus the displacement of the shuttle is shown in the figure below. The values of force output shown on the vertical axis of the figure below indicate the force required to move the shuttle to its original position after the shuttle has been displaced to the corresponding value on the horizontal axis [2]. For a given displacement, the force output may be less than the maximum value shown in the figure below because the value of the force output depends upon the loading conditions.



**Plot of Force Output of Thermal Actuator versus Shuttle Displacement**